# Scanning Tunneling Microscopy and Scanning Tunneling Spectroscopy Studies of Planar and Nonplanar Naphthalocyanines on Graphite (0001). Part 1: Effect of Nonplanarity on the Adlayer Structure and Voltage-induced Flipping of Nonplanar Tin−Naphthalocyanine

**Thiruvancheril G. Gopakumar,* Falk Müller, and Michael Hietschold***

*Chemnitz University of Technology, Institute of Physics, Solid Surfaces Analysis Group, D-09107 Chemnitz, Germany*

*Received: September 28, 2005; In Final Form: January 1, 2006*

The adsorption of base-free naphthalocyanine (Nc), a planar molecule, and tin−naphthalocyanine (SnNc), a nonplanar molecule, on a freshly cleaved highly oriented pyrolytic graphite (HOPG) surface at low sample temperature (50 K) has been studied using a variable-temperature scanning tunneling microscope in ultrahigh vacuum conditions. The planar molecules form large areas of defect-free ordered monolayer with high molecular packing density while the nonplanar molecules show different phases of adsorption with lower molecular packing density. The SnNc adlayers follow the same geometry as the graphite substrate and form pure phases of adsorption with either all molecules in a $Sn^{2+}$ up or $Sn^{2+}$ down geometry. Moreover, a one-dimensional selectivity is observed in still another phase of $Sn^{2+}$ down geometry. Multilayers show a completely different kind of adsorption in each case. Nc molecules show columnar $\pi$-stacking whereas the SnNc molecules exhibit noncolumnar stacking. Distinctly, a voltage-induced flipping of nonplanar tin−naphthalocyanine in the monolayer has been observed which can possibly be applied to single-molecular information storage.

## Introduction

Organic molecules are considered as one of the new building blocks for future nanotechnology. Their tiny size, tunable electrical and optical properties, and their ability to self-organize into various nanostructures fuelled the expectation of a technology based on these tiny objects. Plenty of literature about these molecular self-organized structures shows great interest in the fields of fundamental science and technology.[1−5] The structural varieties of phthalocyanines (Pcs) like metal Pc, subphthalocyanine, diphthalocyanine, naphthalocyanine, and so forth and the possibility to tune their optical and electronic properties make the phthalocyanines a versatile family out of these organic molecules.[6,7] So far, many scanning tunneling microscopy (STM) experiments have been performed with different metal Pcs to understand the adsorption structure and electronic properties of adlayers especially for planar molecules, like CuPc,[8−10] NiPc,[11] FePc,[12] CoPc,[10,12] and so forth, on different substrates. In fact, CuPc is one of the first molecules ever imaged by STM[9] and is a subject of numerous studies. All these studies show the influence of the metal atom on the electronic properties and the adsorption geometry of different kinds of two-dimensional (2-D) assemblies of Pcs on crystalline substrates. The main intermolecular and the molecule−substrate interactions in these molecular systems are noncovalent and of the weak van der Waals type. Due to very weak molecule−substrate interaction, the mobility of these organic molecules on graphite is comparatively high. This mobility of molecules on surfaces opens the possibility to make large areas of defect-free adlayer domains. Moreover, due to the type of interaction, the molecular systems are less perturbed, which is a fundamental aspect useful for molecular imaging. Many efforts have been performed toward immobilization using functionalized molecules and coadsorption with alkane chains.[13,14] However, the effect of molecular geometry has rarely been considered in most of these studies. Yakoyamo et al. investigated the nonplanar adsorption and orientational ordering of porphyrin molecules on a Au(111) surface.[15] Lackinger et al. showed different kinds of adsorption isomers of nonplanar tin−phthalocyanine on the Ag(111) surface.[16] Strohmaier et al. deposited PbPc on $MoS_2$ and observed two different phases of adsorption. The change in molecular contrast at the center was interpreted by the relative position of $Pb^{2+}$ with respect to the substrate.[17] Barlow and Hipps showed a voltage-dependent contrast deviation in the case of nonplanar VOPc in which they describe that the relatively dark contrast at the center is due to the lack of states near the Fermi energy at the oxygen, which is protruding out of the molecular plane.[18] The clear understanding of the effect of geometry of the molecule in the self-organization is still a topic of interest.

In this work, we compare the adsorption of base-free naphthalocyanine (planar) and tin−naphthalocyanine (nonplanar) on a graphite basal plane. In the previous work of our group, Lackinger et al. showed the adsorption geometry of base-free naphthalocyanine on a graphite basal plane.[19] In this work, a defect-free adsorption of Nc molecules over several hundreds of nanometers has been shown. The tunneling voltage-dependent contrast difference shows that molecules such as naphthalocyanines are promising in the field of molecular imaging due to a resolvable difference in the electronic structure of the molecular orbitals near the Fermi level. The study of such large systems can help to explore the field of molecular imaging. Compared with naphthalocyanine (Nc), tin−naphthalocyanine (SnNc) has a nonplanar geometry and hence the $\pi$-electrons, which spread through the molecular backbone, have an unsymmetrical distribution with respect to the molecular plane. These $\pi$-elec-

* To whom correspondence should be addressed. Fax: +49 371 531 3181. E-mail: thiruvacheril.gopakumar@physik.tu-chemnitz.de (T.G.G.). Fax: +49 371 531 3181. E-mail: hietschold@physik.tu-chemnitz.de (M.H.).

10.1021/jp055533e CCC: $33.50 
Published on Web 02/24/2006

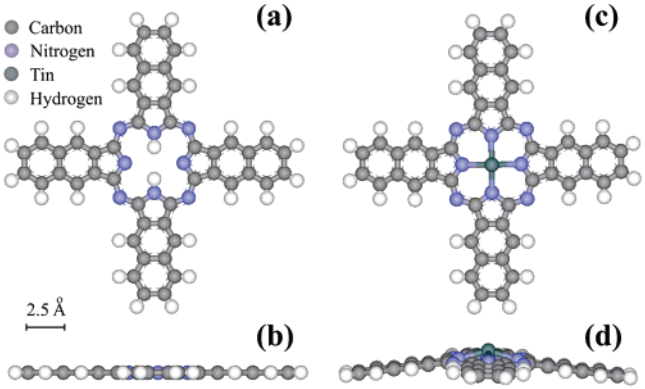


**Figure 1.** Energy-optimized geometrical structures: (a) and (b) show the front and side views of Nc and (c) and (d) show the front and side views of SnNc. In both side views, one of the lateral molecular axes is perpendicular to the plane of the paper.

trons and the protruding $Sn^{2+}$ ion make the system fundamentally and technologically interesting. A possible application for this molecule is to use it as a single-molecular storage device carrying binary information according to the position of the tin atom located on one or the other side of the molecular plane. This article is divided into two parts, part 1 and part 2. In the first part, we discuss the monolayer and multilayer adsorption structures of Nc and SnNc on a graphite substrate and also demonstrate the influence of nonplanarity in the adsorption structure, and finally, we show a voltage-induced flipping of SnNc. In part 2, which is the following article, we compare the current−voltage tunneling spectroscopy of Nc and SnNc.

## Experimental Section

Nc and SnNc have been purchased with a purity of 90% from Aldrich and later cleaned by several cycles of heating in high vacuum and then in ultra-high vacuum (UHV). The monolayers have been prepared by organic molecular beam epitaxy (OMBE) in which the molecules are heated to their evaporation temperature by resistive heating in a Knudsen cell (K-cell). This kind of deposition gives a stable rate of evaporation which is further controlled by a previously calibrated quartz microbalance and by subsequent in-situ STM and low-energy electron diffraction (LEED) measurements. During the deposition, the samples are held at room temperature at a background pressure on the order of $10^{-10}$ mbar. The deposition rate measured by the quartz crystal microbalance is approximately 0.1 nm/min for 8 min from previously degassed molecules. Graphite is freshly cleaved and annealed at 550 °C for 12 h prior to the deposition. Electrochemically etched tungsten tips have been used for the investigation, and all tips have been cleaned by subsequent $Ar^+$-ion sputtering and several heating cycles up to 700 °C. STM experiments have been carried out at a sample temperature of 50 K using a VT-STM from Omicron equipped with a sample cooling by liquid helium flow cryostat. All voltages given with the STM images are referred to the sample.

## Results and Discussion

The energy-optimized geometrical structures of both Nc and SnNc calculated using density functional theory via a Gaussian 98 program package are shown in Figure 1. Parts a and b of Figure 1 are the front and side views of Nc, and parts c and d of Figure 1 are the front and side views of SnNc. Nc has a planar geometry ($D_{2h}$) while the SnNc has a nonplanar geometry ($C_{4v}$) like an umbrella top. Day et al. have shown this by density functional theory calculation in the case of tin−phthalocyanine.[20]

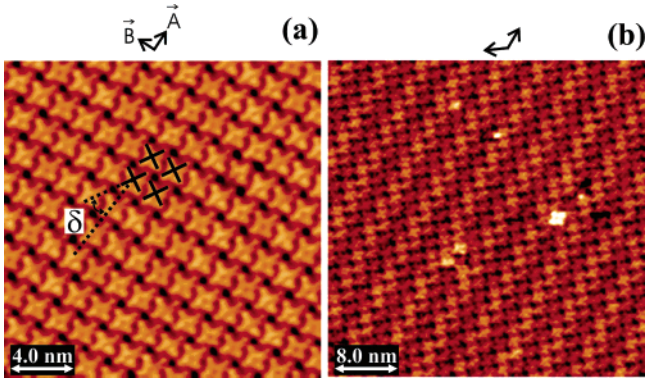


**Figure 2.** STM constant-current topographic images of Nc taken at −1.5 V (a) and −1 V (b) at 90 pA set current. $\delta$ represents the azimuthal angle, and the molecular lattice unit vectors are shown at the top. The vectors shown at the top of (b) are the directions of the contrast modulation.

The planarity change in SnNc is due to the comparatively large ionic radius of the tin atom within the cavity of the Nc backbone. This umbrella top geometry leads to a geometrical isomerism of these molecules on the substrate. The adsorbate molecules may appear in two states, one with metal down and the other with metal up with respect to the substrate surface plane.

**Superstructures of Nc and SnNc.** Figure 2a is the STM constant-current topographic images of Nc on graphite. Nc molecules form an ordered defect-free adlayer, which extends to several hundreds of nanometers with a distorted-square geometry of the unit cell. The relative height profiles and the symmetry of the molecular contrast show that the molecules are adsorbed with their molecular planes parallel to the substrate plane. The crosses in the image represent the position and relative orientation of the molecules within the adlayer. Molecular lattice vectors are marked at the top of the figure, the measured distances are well in agreement with the reported value, $A = B = 1.85 \pm 0.05$ nm, and the angle between the lattice vectors is $96 \pm 1°$.[19] The molecular lattice distances are comparable with the van der Waals radius (∼2 nm) of Nc molecules. Therefore, it is reasonable to assume that the molecules form a close-packed structure with an average packing density of 0.32 molecules/nm$^2$. Lattice distances of different naphthalocyanines on inorganic crystals (RbI, KI, KBr, and KCl) vary from 1.64 nm on RbI to 1.48 nm on KBr and are still smaller when compared with the observed value on HOPG.[21−23] This is presumably due to a commensurate epitaxial growth due to high molecule−substrate interaction, which overcomes the intermolecular steric repulsion and drives the molecules to organize with a tilt angle with respect to the graphite plane. A contrast modulation or Moiré pattern is clearly seen in the large-area scan which is shown in Figure 2b. Directions of this modulation are marked using two arrows at the top of the image. This phenomenon arises due to the nonequivalent adsorption positions of the molecules on the graphite (the molecular adlayer is a noncommensurate superstructure with respect to the substrate lattice).[24,25] This type of molecular epitaxy is referred as point-on-line (coincidence) by Hooks et al. where the growth is considered as energetically less favorable when compared with commensurism.[26] That means the stable adlayer formation is mainly mediated by molecule−molecule interaction. The contrast modulation is used to calculate the exact lattice vectors and the angle between these vectors by fitting the molecular lattice with that of graphite (given in Table 1). The fitting procedure is provided separately in the Supporting Information.

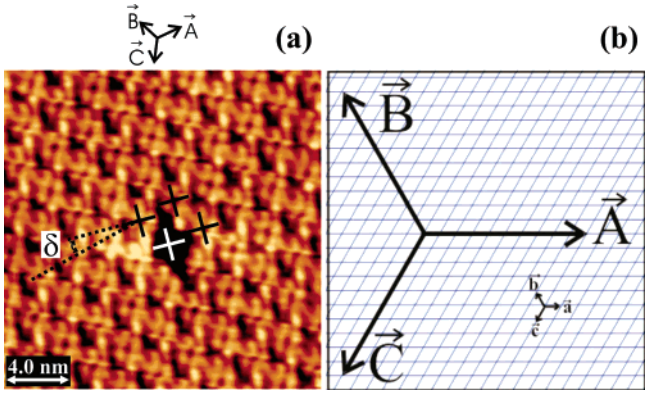


**Figure 3.** (a) STM constant-current topography of SnNc (−1.5 V, 1 nA). $\delta$ represents the azimuthal angle, and the molecular lattice unit vectors are shown at the top. (b) Sketch of the unit cell of SnNc on graphite. $\vec{A}$, $\vec{B}$, and $\vec{C}$ are the molecular lattice unit vectors, and $\vec{a}$, $\vec{b}$, $\vec{c}$ are those of graphite.

SnNc forms defect-free adlayers of quite large area. One of these images is shown in Figure 3a. The adlayer structure shows a very distinct feature in comparison with Nc molecules since there is a hexagonal superstructure with the same geometry as the graphite substrate. The lattice vectors are marked at the top of the figure. These vectors have the same magnitude along all directions and are 2.45 ± 0.05 nm, which is approximately 10 times larger than the lattice vectors of the graphite substrate. Possibly, the molecules form a commensurate lattice with respect to the underlying graphite structure. Figure 3b sketches the proposed commensurate superstructure of SnNc on graphite. $\vec{A}$, $\vec{B}$, and $\vec{C}$ are the molecular lattice vectors, and $\vec{a}$, $\vec{b}$, and $\vec{c}$ are those of the graphite. The lattice vectors are large compared with the van der Waals radius (~2 nm) of the molecules, which means the molecules are not closely packed in the adlayer (average packing density of 0.18 molecules/nm$^2$) compared with Nc. This reveals a relatively weak interaction between the molecules whereas the superstructure geometry reveals a stronger interaction between the molecules and the substrate.

It is well-known that for molecular self-assemblies the interactions are mainly of the weak and reversible noncovalent types such as van der Waals, electrostatic, and hydrogen bonds.[27] In the case of metal phthalocyanines, the main intermolecular interactions are the van der Waals attraction between the $\pi$-electron systems and the repulsive steric constraints between the molecules. Molecule−substrate interaction is a partial metallic bonding between the central metal atom and the semimetallic graphite surface. To consider a weak intermolecular interaction in the case of a SnNc molecule is likely due to the unsymmetrical $\pi$-electrons (nonconstructive interaction), which arise due to the nonplanar geometry ($C_{4v}$ symmetry of SnNc). This is not the case in the planar Nc molecule, and hence, a stronger molecule−molecule interaction can be expected between them. Moreover, the hydrogen atoms in the nuclei of the Nc molecules reduce the molecule−substrate interaction. On the other hand, the single-point metal contact increases predominantly the molecule−substrate interaction in SnNc, which is supported by the observed superstructure geometry (hexagonal) similar to that of the graphite substrate.

To understand the factors affecting the packing density, one has to consider the azimuthal orientation of the molecules (the smallest angle between one of the molecular axes and the lattice vector of molecular adlayer). In Figures 2a and 3a, $\delta$ represents the azimuthal angle which is smaller in the case of the SnNc adlayer ($\delta \approx 14 \pm 2°$) compared with that of the Nc adlayer ($\delta \approx 28 \pm 1°$). The azimuthal angle defines the steric construction within the adlayer, that is, how the molecules are oriented with respect to each other. If $\delta$ is large, then the molecular lobes are far apart and feel less steric repulsion from the neighboring molecular lobes in the adlayer. This favors an interdigitation of molecules, and hence, a close-packed adlayer structure is possible. When the azimuthal angle is smaller, the molecular lobes are close to each other and hence a hydrogen steric repulsion between the molecular lobes is to be expected. The molecules arrange themselves in an equilibrium position of adsorption with larger intermolecular distance (smaller packing density). Thus, a strong molecule−molecule interaction and a weak molecule−substrate interaction lead to the formation of close-packed superstructures with larger azimuthal angles, like those in the Nc adlayers. In contrast, a weak molecule−molecule interaction and azimuthal orientation (smaller azimuthal angle) lead to a loosely packed adlayer, which is the case in SnNc where high molecule−substrate interactions also have to be considered. Table 1 shows the comparison of the adlayer structures of Nc and SnNc on the graphite basal plane.

**TABLE 1: Comparison of the Adlayer Structure of Nc and SnNc on a Graphite Basal Plane**

| | Nc@graphite | | SnNc@graphite |
|---|---|---|---|
| | Experiment | Contrast Modulation Fitting* | |
| Lattice vector, $\vec{A} \approx \vec{B}$ | 1.85 ± 0.05 nm | 1.927 nm | 2.5 ± 0.05 nm |
| Angle between lattice vectors | 96 ± 2 ° | 96.103 ° | 60 ± 2 ° |
| Matrix representation of molecular lattice vector[26] ** | $\begin{bmatrix}\vec{A}\\ \vec{B}\end{bmatrix} = \begin{bmatrix}7.833 & 0\\ -5.329 & 8.992\end{bmatrix}\begin{bmatrix}\vec{a}\\ \vec{b}\end{bmatrix}$ | | $\begin{bmatrix}\vec{A}\\ \vec{B}\end{bmatrix} = \begin{bmatrix}10 & 0\\ 0 & 10\end{bmatrix}\begin{bmatrix}\vec{a}\\ \vec{b}\end{bmatrix}$ |
| Adlayer Structure | Distorted Quadratic | | Hexagonal |
| Azimuthal angle ($\delta$) | 28 ± 1° | | 14 ± 2° |
| Packing density | ≈ 0.32 molecules/nm$^2$ | | ≈ 0.18 molecules/nm$^2$ |

*These values are elucidated by a trial and error fitting method of molecular lattice on graphite lattice, which is illustrated in the Supporting Information. **$\vec{a}$ and $\vec{b}$ are the unit lattice vectors of graphite.

**Pure Phases of SnNc.** In STM, the molecular contrast arises from the local density of states (LDOS) of molecules near the Fermi energy. In the case of different metal phthalocyanines, NiPc, CuPc, FePc, and CoPc, Hipps et al. showed apparent depression and protrusion according to the metal ions in the center.[11,12] Lackinger et al showed a highest occupied molecular orbital−lowest unoccupied molecular orbital (HOMO−LUMO) switching with respect to the applied sample bias.[19] Therefore, to understand the adsorption and the electronic structure of molecules on a substrate, it is necessary to know the molecular orbital symmetry of filled and unfilled levels near the Fermi energy. Figure 4 shows the energy level diagram of SnNc near the Fermi energy (a) and the symmetry of the HOMO ($A_2$) (b), HOMO − 1 ($A_1$) (c), and one of the degenerate LUMOs (2e) (e) viewed from the side of the $Sn^{2+}$ ion. The symmetry of HOMO − 1 ($A_1$) (d) viewed from the opposite side of the $Sn^{2+}$ ion and one of the degenerate LUMOs (2e) (f) viewed from the side are also included in the figure. The calculation is done using Gaussian 98 with the B3LYP/LANL2DZ basis set. The energy level diagram shows the HOMO−LUMO gap and the difference in energy between HOMO to HOMO − 1 and degenerate LUMOs to LUMO + 2. The molecular orbital symmetry of the HOMO shows that the electron density arises mainly from the $\pi$-electrons, which spread through the molecular skeleton, and there is observed no contribution from the central metal ion. Interestingly, HOMO − 1 shows an electron density

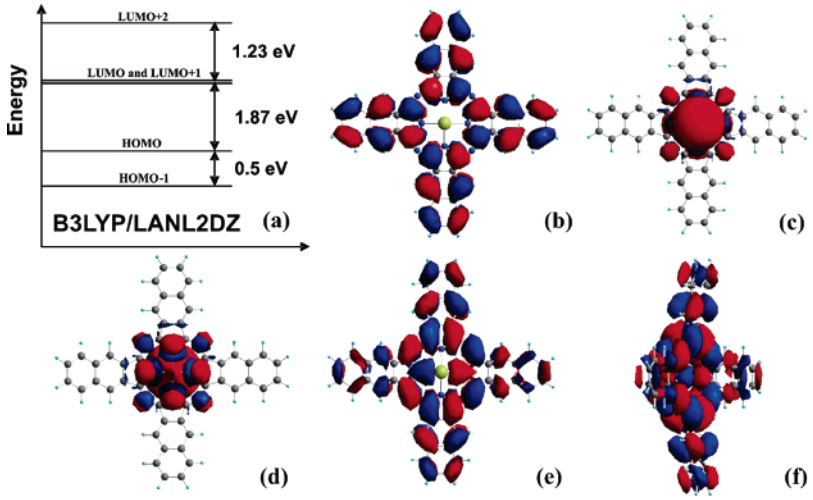


**Figure 4.** Energy level diagram of SnNc (a) and the symmetry of HOMO ($A_2$) (b), HOMO − 1 ($A_1$) (c), and degenerated LUMOs (2e) (e) viewed from the side of the $Sn^{2+}$ ion. The symmetry of HOMO − 1 ($A_1$) (d) viewed from the opposite side of $Sn^{2+}$ ion and the side view of degenerated LUMOs (2e) (f). Calculation was performed using Gaussian 98 with the B3LYP/LANL2DZ basis set.

which arises mainly from the central metal atom. The electron density of this orbital can be understood from the electronic configuration of $Sn^{2+}$ ([Kr] $5s^2$ $4d^{10}$ $5p^0$). The filled d and s orbitals in the outermost level of $Sn^{2+}$ contribute to the high electron density at the center of the molecule. Moreover, the electron density is protruding out of the molecular plane only on the side of metal ion, and the opposite side of HOMO − 1 appears as a valley (shown in Figure 4d). The electron densities of LUMO and LUMO + 1 have similar spatial symmetry when rotated by 90° and are degenerated in energy. The symmetry of these orbitals shows that it arises from the $\pi$-electrons. Even though in contrast to the HOMO, they have an additional electron density near the center which originates presumably from the atomic non-s states. This makes the center of the molecular orbital rich in electron density and appears as a protrusion, however, the opposite side appears as a valley due to the nonplanar structure of the molecule (shown in Figure 4f). The gap between HOMO and HOMO − 1 (0.5 eV) is relatively small, to resolve in the STM image, in comparison with that of the LUMOs and LUMO + 2 (1.23 eV). Then it is reasonable that the molecular contrast can be a convolution of both HOMO and HOMO − 1 at a negative sample bias, but the molecular contrast is only from the LUMOs at a positive sample bias. Therefore, if the molecule has a $Sn^{2+}$ ion-down adsorption, at both positive and negative sample biases, then the molecular contrast should be similar and show a depression, that is, low topographic contrast at the center. In $Sn^{2+}$ ion-up adsorption, at both sample biases, the center of molecular contrast should appear as a bright protrusion.

As expected, we found two different phases of adsorption with respect to the relative position of the $Sn^{2+}$ ion for SnNc molecules when they adsorb onto the substrate plane. Figure 5 shows these different phases of adsorption. Phase I which is shown in parts a and b of Figure 5 is a pure phase. Single molecules appear as bright protrusions, one such molecule is marked with ring. The single-molecule point defects, also seen in the images and indicted by arrows, could be used to identify the position of single-molecule adsorption. Images taken at positive and negative sample biases show a similar appearance in their contrast, especially at the center. The degenerate LUMOs and HOMO − 1 have a high contribution of electron density near the center when viewed from the side of the metal ion. So it is reasonable that the molecular contrast corresponds to a $Sn^{2+}$ ion-up adsorption geometry.

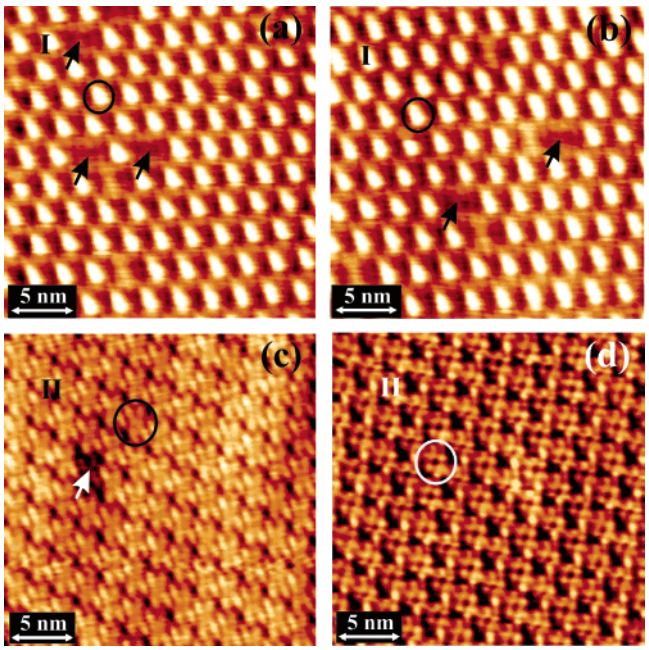


**Figure 5.** STM constant-current topography images of SnNc on graphite: (a) and (b) are images of phase I taken at positive and negative sample biases (1.5 V), respectively, with a set current of 250 pA; (c) and (d) are images of phase II taken at positive and negative sample biases (1.5 V), respectively, with a set current of 250 pA (c) and 1 nA (d). Arrows show the positions of missing single molecules.

Phase II which is shown in parts c and d of Figure 5 is also a pure phase. Single molecules are marked with rings and appear with a relatively low intensity at the center for both positive and negative sample biases. Especially the image at the negative sample bias shows a very clear, dark appearance at the center, which could be attributed to the appearance (orbital electron density) of the HOMO and HOMO − 1 from the opposite side of the $Sn^{2+}$ ion. The image at the positive sample bias can be assigned to the degenerated LUMOs which have no electron density at the center when viewed from the opposite side of the metal ion. This justifies that the molecular contrast with low tunneling probability at the center corresponds to $Sn^{2+}$ ion-down adsorption geometry. Very rarely in the scanning have we found either of these pure phases with defects especially in the adsorption isomers. It is likely that in a pure phase the

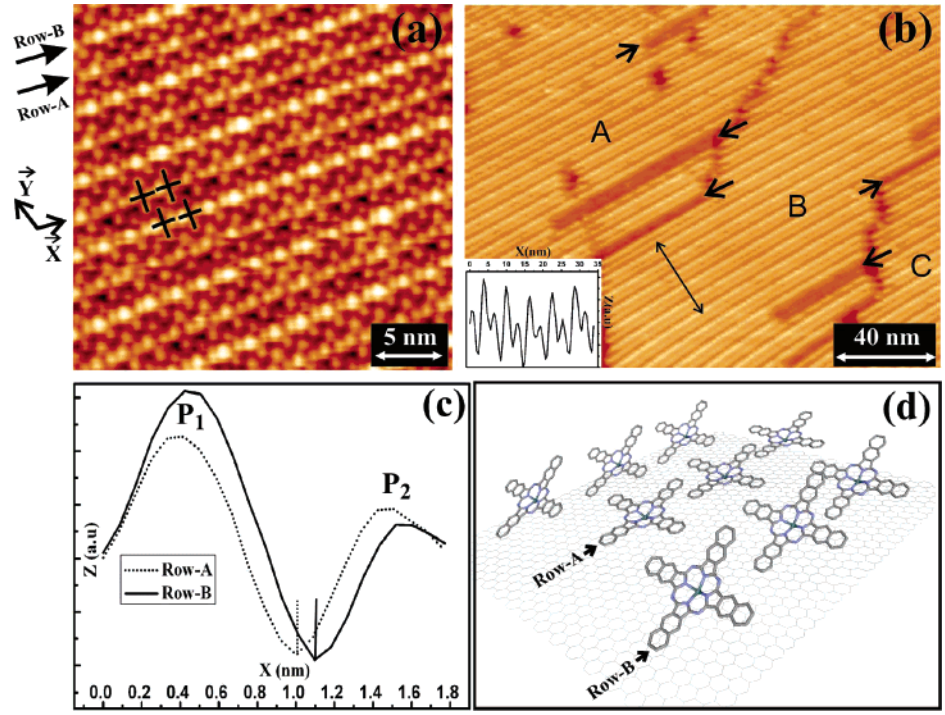


**Figure 6.** (a) and (b) show the STM constant-current topography of the 1-D phase (phase III) taken at different magnifications (−1.5 V, 200 pA). (a) Different rows are marked as row A and row B, the molecular lattice directions are marked as $\vec{X}$, and $\vec{Y}$, and crosses depict the single molecules. (b) The inset includes the line profile along the double-headed arrow, and the arrows show the line defects. A, B, and C are different domains. (c) Averaged line profile of 15 molecules from each row along the *X* direction: the dotted line represents the molecule in row A and the solid line the molecule in row B. (d) Qualitative model which shows the perspective view of molecular rows A and B.

intermolecular interactions are more effective compared with that in a defective phase and the molecules try to be in an equilibrium true phase. Moreover, the similar lattice parameter and the adsorption structure (hexagonal geometry) as well as the predicted commensurate superstructure lead to a reasonable explanation that in both phases molecules have the same adsorption sites even though the adsorption isomers are different. So it is reasonable that the molecules have an equilibrium state of adsorption in any of these pure phases. Similar equilibrium states of pure phases were found in the case of nonplanar PbPc.[17]

**One-Dimensional Phase in SnNc.** Besides the above-mentioned phases, an additional more interesting phase (phase III) is found in which the molecules show a one-dimensional (1-D) selectivity in the self-organization. Suto et al. found a 1-D selectivity in the organization of mixed adsorption of copper tetraphenyl porphyrine (CuTPP) and cobalt phthalocyanine (CoPc) on Au(111) and Au(100) surfaces.[28] STM constant-current topography of phase III from SnNc is shown in Figure 6a. The molecular lattice directions are marked as $\vec{X}$ and $\vec{Y}$. The molecules in this phase show a different kind of adsorption in adjacent rows and a preferred orientation along one of the molecular lattice directions. This can be seen from the difference in contrast between the adjacent rows of molecules along the $\vec{Y}$ direction. Different rows are marked as row A and row B in which row B looks relatively brighter than row A. In the large-area scan, the contrast difference between the adjacent rows is distinguishable, which is shown in Figure 6b. The inset of this figure is the topographic profile along the double-headed arrow; it shows the height difference between adjacent rows (the relative values between adjacent peaks are used and not the absolute values). The figure shows two domain boundaries separating the domains A, B, and C from each other, which are presumably due to the different initial states (nucleation positions), on a single HOPG domain, which then continues and meets at these domain boundaries. More interesting are the linear defects indicated by arrows, which are characteristic due to their preferred direction, that is, along the direction of the 1-D structure. This is likely because the defect can still preserve the symmetry of organization and thereby the 1-D chains are undisturbed. In the defect-free areas, we have observed chains of more than 200 nm length.

The crosses in Figure 6a depicting the single molecules show that one of the molecular axes is aligned along the molecular lattice direction $\vec{X}$. Each molecular pattern has four lobes; one of them is comparatively brighter than the others in both rows. However, the relative intensity of this molecular lobe is low in row A, which makes the contrast between the adjacent rows different. Figure 6c is the averaged line profile of more than 15 molecules from each of the rows along one of the molecular axes ($\vec{X}$). The relative values of height profiles were used for comparison. The dotted line represents the average topographic profile of molecules in row A, and the solid line corresponds to that of the molecules in row B. Both line profiles have two intense peaks ($P_1$ and $P_2$) with a minimum at the center of the molecule. That means in both rows the molecules have tin ion-down geometry (discussed in the Pure Phases of SnNc section). The relative intensity ratio, $P_1/P_2$, is greater than the one in both curves, which indicates that the molecules are tilted toward graphite along the molecular axis direction $\vec{X}$. However $P_1/P_2$ of the solid curve is larger compared with that of the dotted line. This suggests that the molecules in row B are tilted steeper toward the graphite surface than the molecules in row A. In contrast to the above-mentioned pure phases (phases I and II), the measured lattice constant between the molecules in the $\vec{X}$-direction ($2.1 \pm 0.1$ nm) is smaller compared with that of the molecules in the $\vec{Y}$-direction ($2.5 \pm 0.1$ nm). The whole molecular geometry of the unit cell however follows a stretched hexagonal structure. Therefore, it is likely that the molecular organization is influenced by the substrate geometry presumably due to a strong molecule−graphite interaction as discussed

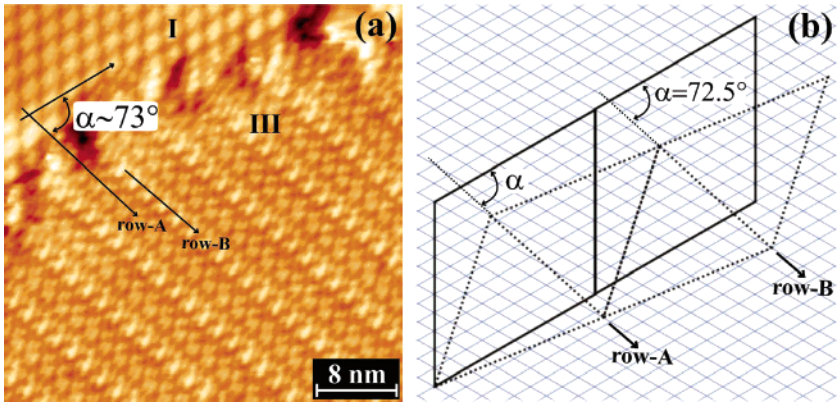


**Figure 7.** (a) STM constant-current topography of SnNc on graphite (1.3 V, 120 pA), different phases are marked as I and III. (b) Geometrical model for the molecular superlattice of phase I (solid line) and phase III (dotted line) on graphite. α is the angle between one of the lattice vectors of phase I and the 1-D chain structure in phase III.

above for the adsorption structure of phases I and II. The preferred direction of the defects (line defects) along the 1-D structure proves that this is a real topographic and orientational effect of molecules which cannot be mimicked to any kind of drift or distortions in the images. Such a 1-D selectivity in the adsorption has not been observed in the planar derivative Nc[19] as well as the smaller nonplanar SnPc[29] on graphite, that is, the observed phase III is the effect of both the extended molecular lobes and the nonplanar geometry of SnNc (which makes the molecule more nonplanar in nature compared with SnPc).

For a better understanding of this selectivity in the self-organization, we have proposed a qualitative model on the basis of molecular orientations with respect to each other. The crosses in Figure 6a depict the molecular orientation. It is seen that one of the molecular axes is collinear with respect to the same of the neighboring molecule along the $\vec{X}$-direction. Then it is likely that the molecules feel a steric repulsion between each other due to the hydrogen atoms at the edges of the molecular lobes, that is, the molecules are tilted toward the substrate in the $\vec{X}$-direction so that the mean distances between the hydrogen atoms increase and thus change to a stable adsorption. This tilt makes the topography of one of the molecular lobes higher compared with the other lobes and appears as a bright feature in the STM images. This tilt brings the molecules closer, and hence, a better molecule−molecule interaction can be expected. This can be concluded from the small unit lattice vector along the $\vec{X}$-direction. Figure 6d is the qualitative model, which shows the perspective view of three molecular rows. The relative tilt in each row can be clearly seen, and the corresponding rows are marked.

Figure 7a shows a domain boundary between phase I and phase III. The rotation angle, α, between one of the lattice vectors in phase I and the 1-D structure ($\vec{X}$-direction) in phase III is 73 ± 1°. The angle between the domains shows that these are clearly different phases arising due to different adsorptions on the substrate and are not just rotational domains of a single phase. Figure 7b is the geometrical model for the molecular superlattice of phase I (solid lines) and phase III (dotted lines) on graphite. Phase I is a commensurate superstructure on the graphite substrate as mentioned in the first section of this article. The proposed model for phase III is obtained by taking into account α and the unit lattice vectors measured in the images. The model shows good agreement with the experimental observations. The difference in the tilt angles of the molecules to substrate, although the molecular orientation is similar in both rows, arises due to the difference in adsorption sites, that is, the molecules in the intermediate rows have a commensurate

**SCHEME 1. Summary of Different SnNc Phases on HOPG**

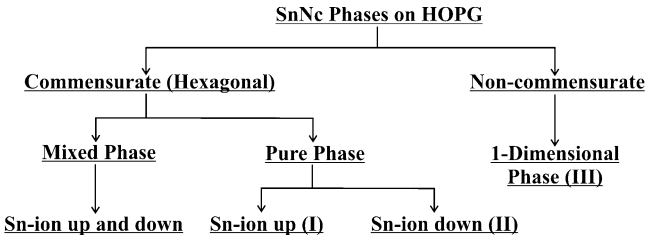


geometry with the graphite along the $\vec{Y}$-direction. Therefore, the adsorption geometries of row A and row B are different and appear as a different contrast. The different kind of molecular tilt orientation in the molecular lattice forms an ABAB-like packing along the $\vec{Y}$-direction. Moreover, AA or BB repeating units are never observed, so it can be deduced that the molecular tilt orientation depends on the adsorption sites. However, in row A, several defects were observed with molecules having tilt in the opposite direction and molecules which are not tilted at all. These results show that the adlayer structure depends on the relative orientation of the molecules, and moreover, the 1-D chainlike structure proofs for the first time the effect of nonplanarity and hydrogen−hydrogen steric repulsion in the adsorption geometry of naphthalocyanine.

However, the exact reason for the molecules to orient with their molecular lobes parallel to each other could only be understood by the theoretical simulation of molecules on the graphite surface, which certainly needs some efforts using molecular-dynamic concepts. A summary of all observed phases of SnNc on HOPG is shown in Scheme 1.

**Multilayer Structures of Nc and SnNc.** Multilayer structures of Nc and SnNc on graphite have been of interest especially in the adsorption structure due to the geometry of the molecules. Parts a and b of Figure 8 show the STM constant-current topography of Nc molecules at different magnifications. The brighter contrasts which are indicated by arrows in Figure 8a are the single Nc molecules and dimers adsorbed above the first layer. These molecules are found stacked into a columnar packing where the molecules in the second layer adsorb exactly on top of the underlying ones. Crosses depict the azimuthal orientation of the molecules in the first and second layers. Azimuthal orientation shows that both molecules have the same adsorption geometry in the first and second layers. The exact adsorption geometry of the molecules can be understood from the high-resolution pictures. Figure 8b shows a high-resolution picture of an Nc molecular adlayer. As discussed in the previous

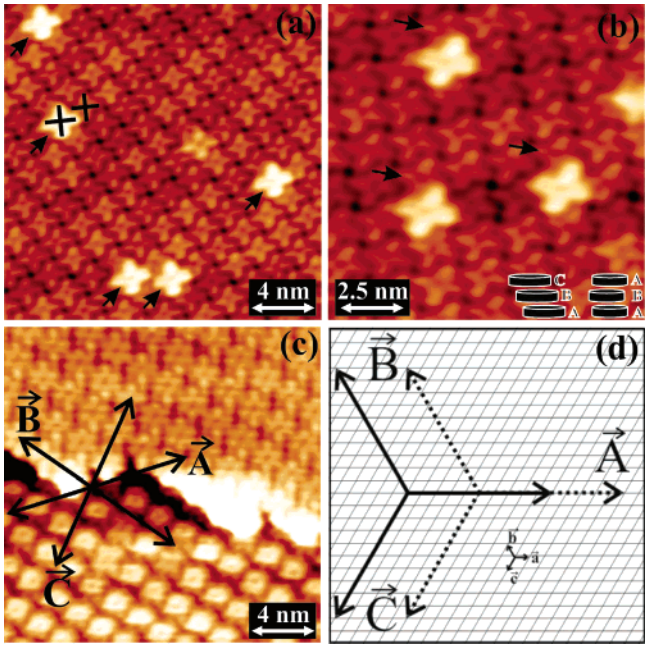


**Figure 8.** (a) and (b) STM constant-current topography of Nc with single molecules in the second layer (−1.2 V, 100 pA). The inset in (b) is the cartoons of multilayer packing. (c) The STM topographic image of the SnNc multilayer (−1.5 V, 1 nA). (d) The possible multilayer geometry of SnNc: $\vec{A}$, $\vec{B}$, and $\vec{C}$ are the molecular unit lattice vectors, and $\vec{a}$, $\vec{b}$, and $\vec{c}$ are those of graphite; the dotted arrows represent unit vectors of the first layer, and the solid arrows correspond to those of the second layer.

picture, the bright molecular contrast corresponds to the molecules in second layer. The neighboring molecules in the first layer of these single molecules (second layer) have a different appearance. The molecules which are marked using arrows are not completely visible compared with the other three molecules. This tells us that the molecules in the second layer are not adsorbed exactly on the top of the molecules in first layer, instead they are packed into columns with an offset center, although all molecules have the same orientation in different layers, that is, the center of the molecules is not aligned straight along the *z*-axis. The inset of Figure 8b shows two possible columnar packings of the molecules with respect to the substrate. It is known from the literature that there are columnar and noncolumnar stackings of planar phthalocyanine molecules and PTCDA especially in the bulk phases.[30−32] $\pi-\pi$ stacking mainly occurs via two different kinds of $\pi$-electron cloud interactions. One is a face-to-face interaction in which both molecules have their molecular planes ($\pi$-electron clouds) parallel to each other.[33] The second molecule however has an off-center compared with that of the first one, which has a constructive interaction like in the case of graphite.[32,33] The second interaction is an edge-to-face where the second molecule interacts perpendicular to the molecular plane ($\pi$-electron cloud) of the first.[33−37] So it is reasonable that planar Nc molecules with relatively large $\pi$-systems can form columnar ($\pi$-stacking) adsorption in the multilayers. The packing of a closed second adlayer can be considered as the replication of this single molecular adsorption, which produces ABAB (columns) or ABCD (tilted columns) like packing along the *z*-axis as shown in the inset of Figure 8b. However, it is not really clear which situation is encountered in the Nc multilayer due to the lack of experimental data.

Figure 8c shows the constant-current topography of SnNc where the first (lower half of the image) and second (upper half of the image) layers are clearly seen. In this case, we found

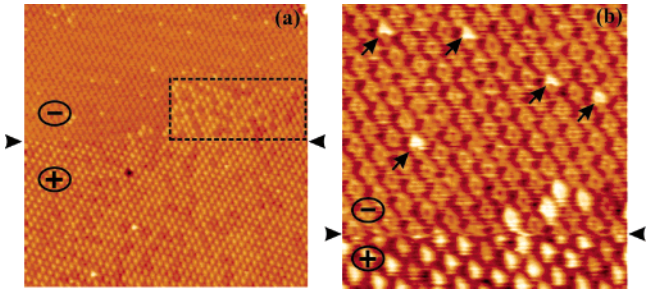


**Figure 9.** STM constant-current topographic images of SnNc on graphite: (a) 100 × 100 nm$^2$, |2| V, and 300 pA and (b) is a 30 × 30 nm$^2$ area zoom of the same image. Arrowheads in both cases indicate the line at which the voltage has been reversed. In both images, scanning proceeds from bottom to top.

areas with completely packed second layers. Double-headed arrows depicting the orientation of superlattice and crystallographic directions on the substrate are marked as $\vec{A}$, $\vec{B}$, and $\vec{C}$. Both layers show the same kind of hexagonal structure, but the molecules in the second layer are located above the voids of the first layer (shifted half of the molecular lattice vector), meaning the molecules viewed along the lattice vectors $\vec{B}$ and $\vec{C}$ show an ABAB-like packing in the *z*-axis and the molecules viewed along the lattice vector $\vec{A}$ show an AAAA-like packing in the *z*-axis. Figure 8d shows the possible adsorption sites of molecules in the first (solid line) and in the second (dotted line) layers. $\vec{A}$, $\vec{B}$, and $\vec{C}$ are the molecular unit lattice vectors. This is an interesting effect in comparison to the Nc molecules that the $\pi$-stacking tendency was lost due to the nonplanar geometry, that is, to have a constructive interaction of the $\pi$-electrons with the $p_z$ orbitals which are perpendicular to the molecular plane, they have to overlap face-to-face (along the molecular plane) which is not the case in the umbrella top symmetry of SnNc.

**Voltage-induced Flipping of SnNc.** The most interesting effect found in SnNc is a voltage-induced flipping of molecules from one adsorption state to the other. That is, the $Sn^{2+}$ ion position switches from one side to the other with respect to the molecular plane. Yanagi et al. showed a STM-induced dynamical flip-flop switching of nonplanar subphthalocyanine ("chloro-[subphthalocyaninato]-boron(III)") on Cu(100).[38] Figure 9a depicts such a voltage-induced flipping of SnNc molecules. Arrowheads show the line at which the ramp potential has been switched, and the corresponding voltage signs of the frame after and before switching are shown. The lower part of the figure shows approximately 90% of the molecules in a $Sn^{2+}$ ion-up position and the remaining 10% in a $Sn^{2+}$ ion-down position. After switching the sample bias from a positive to negative value, almost 100% of the molecules flip from their $Sn^{2+}$ ion-up geometry to a $Sn^{2+}$ ion-down geometry, except for the region marked in a rectangular box (see the upper half of the image). This shows that the molecules initiate themselves to a completely pure phase (all molecules to a $Sn^{2+}$ ion-down geometry). However, immediately after switching the potential, several molecules (marked within the dotted square) may also remain unchanged in their geometry. This observation confirms that the phenomenon is a dynamical flipping and not a tunneling voltage-dependent contrast difference (for example, HOMO−LUMO imaging). So the molecules show a tendency to flip from one adsorption phase to the other, which is a pure phase of molecules with either $Sn^{2+}$ ion-up or ion-down position. The existence of pure phases of adsorption (phase I and phase II) has been discussed in the previous section. The effect of flipping is a collective effect which depends on the adsorption state of neighboring molecules. That is, the adsorption state of each

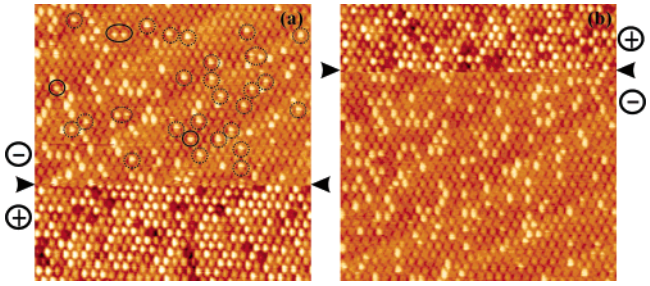


**Figure 10.** (a) and (b) are 75 × 75 nm$^2$ STM constant-current topographic images of SnNc on graphite taken at |2| V and 1000 pA. Arrowheads in both cases are the line at which voltage has been reversed. The scan direction is from bottom to top.

molecule forces the neighboring molecules to switch to the same adsorption state when the voltage switches from one sign to another ("a self-repairing molecular superstructure"). This effect is clear from the unflipped region marked with a dotted rectangle. The unflipped region has nearly 60% of its molecules with a $Sn^{2+}$ ion-up state which is nearly an intermediate state for the molecular clusters to go to either of its true phases. Presumably, the molecule forces the neighboring molecules and then flips completely into the $Sn^{2+}$ ion-down state during the rest of scanning. However, the molecules in the $Sn^{2+}$ ion-down geometry before the voltage switching (10% of the molecules with a $Sn^{2+}$ ion-down state at the lower part of the image) did not show an inverse flipping and remain in the same adsorption state. That is, the molecules remain in one of the pure phases. The molecules which change their adsorption states during the scanning are shown in Figure 9b (indicated by arrows), which is a zoom from Figure 9a. The bright contrasts appearing from the middle of scanning at these molecules (the scan direction is from bottom to top) are those which flipped from a $Sn^{2+}$ ion-down position to a $Sn^{2+}$ ion-up position after the switching of potential. Presumably, this is the inverse flipping of those molecules which were already in the $Sn^{2+}$ ion-down position before the voltage switching. This image differentiates the contrast at the center of molecules at different polarities and thus confirms the relative positions of the $Sn^{2+}$ ions at different regions of the scan. The phenomenological fact behind the flipping phenomena can be understood from the dipole moment and its orientation within the molecule. The calculated (B3LYP/LANL2DZ) dipole moment ($\vec{P}$) is 1.48 D along the *z*-axis (perpendicular to the molecular plane). On the other hand, $\vec{P}$ is zero in the planar Nc molecule. This suggests that the spatial separation of the electropositive metal atom from the backbone of the molecule creates a high dipole moment along the *z*-axis. Then it is reasonable that the positive center ($Sn^{2+}$) is stabilized in the negative potential field. Thus, the molecules with $Sn^{2+}$ ion-up position flip to $Sn^{2+}$ ion-down geometry when the sample bias switches from positive to negative. The flipping energy of molecules from one to another adsorption state can be roughly estimated as the product of the dipole moment of molecules and the applied field, $E_{\text{flipping}} = -\vec{P}\vec{E}_{\text{field}}$, which is approximately −1.5 eV (calculated for a tunneling distance of 1 nm). This value shows that the flipping is influenced by the applied field and excludes a thermal excitation, which has been observed.

To understand the effects which influence this, we carried out the experiment in a more mixed phase (meta phase) of $Sn^{2+}$ ion-up (≈ 40%) and -down (≈ 55%) positions. Figure 10 shows the consecutive images of such a mixed phase which have been imaged with both positive to negative and negative to positive potential switching. Immediately after switching the potential, more than 80% of the molecules show $Sn^{2+}$ ion-down geometry (upper part of the image) even though many molecules switch their contrast during the rest of scanning in which most of the molecules flip from $Sn^{2+}$ ion-down to an up state. These kinds of molecules are marked inside the dotted circles, and the flipping of a few molecules from $Sn^{2+}$ ion-up to the down state is depicted by the solid circles in Figure 10a. Thus, in a relatively unstable (nonequilibrium) mixed phase, the molecules always try to switch back and forth when influenced by a voltage polarity switching. Such phenomena may continue until the molecules find the equilibrium state. But the effect of a decreased tip sample distance (high set current) cannot be excluded as one of the reasons for these increased random flippings of molecules. The phenomenon may depend not only on a single reason like voltage switching but also on the nonequilibrium phase and the decreased tip sample distance. However, in a completely pure phase, we found the flipping and inverse flipping of all SnNc molecules by the reversal of the sample bias without any intermediate stages or random flipping. This indicates that in a pure phase the molecules behave as a group so that the stable adsorption geometry is undisturbed. The random flipping tendency in a mixed phase and the complete flipping in the pure phase confirm that the molecule favors a pure adsorption phase that is either $Sn^{2+}$ ion-up or down. This reversible flipping phenomenon possibly recommends this molecule as a single-molecule memory application according to the position of the $Sn^{2+}$ ion located either on one side (1) or on the other (0) with respect to the molecular plane, working at an information density of approximately 50 Tbit cm$^{-2}$. An information density of 60 Tbit cm$^{-2}$ is predicted in the case of subphthalocyanine, where the memory application works on the basis of a dynamical flip-flop mechanism.[38] Considering an ultrafast (picoseconds or more) quantum mechanical tunneling phenomenon (flipping) of nonplanar umbrella top SnNc over the kinetic process (dynamic flip-flop) would lead to very fast (Tbit/s or more) computing efficiencies. But to consider this as a real application base, there are challenges such as (1) selectivity of flipping over the desired molecules (this allows a printing in the molecular scale), (2) high reversibility of the process (which has been partially shown), and (3) thermal stability (which seems to be established due to the high-flipping energy barrier between the two adsorption states).

## Conclusions

Planar Nc and nonplanar SnNc have been investigated using a variable-temperature STM. Nc molecules form a close-packed adlayer structure while SnNc forms a loosely packed adlayer. In the case of Nc, a strong molecule−molecule interaction and a weak molecule−substrate interaction lead to the formation of close-packed adlayers. In contrast, a weaker molecule−molecule interaction and the azimuthal orientation (smaller azimuthal angle) lead to a loosely packed adlayer in the case of SnNc where strong molecule−substrate interactions become the deciding factor. Compared with planar Nc, the nonplanar molecules show different phases of adsorption due to two geometrical isomers, with metal ion-up and down positions. Pure phases of these two isomers on graphite are found. In a pure phase, the intramolecular interactions are more effective compared with those in a defective phase and the molecules try to be in one of the equilibrium pure phases. Moreover, the similar lattice parameter and the adsorption structure (hexagonal geometry) in both cases and the predicted commensurate superstructure lead to a reasonable explanation that in both phases molecules have the same adsorption site even though

the adsorption isomers are different. So it is to be assumed that the molecules have equilibrium states in both of these pure phases. Besides the pure phase, a 1-D chain structure has been observed. This 1-D structure reveals the crucial effect of molecular orientation in the adlayer structure and the effect of nonplanarity and hydrogen−hydrogen steric repulsion in the adsorption geometry of naphthalocyanines. Adsorption of multilayers shows a columnar $\pi$-stacking in Nc molecules whereas the SnNc molecules show noncolumnar stacking. A voltage-induced flipping phenomenon has been found in the case of nonplanar SnNc, which shows that the molecules prefer to be in an equilibrium pure phase of adsorption. The reversibility of this process enables a possible application of these molecules for a memory application as a single-molecule storage device with an information density of 50 Tbit $cm^{-2}$.

**Acknowledgment.** T.G.G. thanks the "Deutsche Forschungsgemeinschaft" for financial support within the Graduate College "Accumulation of Single Molecules to Nanostructures".

**Supporting Information Available:** Elucidation of the superstructure unit lattice vector and the angle between the lattice vectors from the contrast modulation. This material is available free of charge via the Internet at http://pubs.acs.org.

## References and Notes

(1) Yokoyama, T.; Yokoyama, S.; Kamikado, T.; Okuno, Y.; Mashiko, S. *Nature* **2001**, *413*, 619.

(2) (a) Hipps, K. W.; Scudiero, L.; Barlow, D. E.; Cooke, M. P., Jr. *J. Am. Chem. Soc.* **2002**, *124*, 2126. (b) Scudiero, L.; Hipps, K. W.; Barlow, D. E. *J. Phys. Chem. B* **2003**, *107*, 2903.

(3) Böhringer, M.; Morgenstern, K.; Schneider, W.-D.; Berndt, R.; Mauri, F.; De Vita, A.; Car, R. *Phys. Rev. Lett.* **1999**, *83*, 324.

(4) Griessl, S. J. H.; Lackinger, M.; Jamitzky, F.; Markert, T.; Hietschold, M.; Heckl, W. M. *J. Phys. Chem. B* **2004**, *108*, 11556.

(5) (a) Yablon, D. G.; Wintgens, D.; Flynn, G. W. *J. Phys. Chem. B* **2002,** *106*, 5470. (b) Wei, Y.; Kannappan, K.; Flynn, G. W.; Zimmt, M. B. *J. Am. Chem. Soc.* **2004**, *126*, 5318.

(6) Inabe, T.; Tajima, H. *Chem. Rev.* **2004**, *104*, 5503.

(7) Collins, R. A.; Mohammed, K. A. *J. Phys. D: Appl. Phys.* **1988**, *21*, 154.

(8) Lippel, P. H.; Wilson, R. J.; Miller. M. D.; Wöll, Ch.; Chiang, S. *Phys. Rev. Lett.* **1989**, *62*, 171.

(9) Gimzewski, J. K.; Stoll, E.; Schlittler, R. R. *Surf. Sci.* **1987**, *181*, 267.

(10) (a) Yoshimoto, S.; Tada, A.; Suto, K.; Itaya, K. *J. Phys. Chem. B* **2003**, *107*, 5836. (b) Suto, K.; Yashimoto, S.; Itaya, K. *J. Am. Chem. Soc.* **2003**, *125*, 14976.

(11) Xing, Lu.; Hipps, K. W. *J. Phys. Chem. B* **1997**, *101*, 5391.

(12) Hipps, K. W.; Xing, Lu.; Wang. S. D.; Mazur, U. *J. Phys. Chem. B* **1996**, *100*, 11207.

(13) (a) Qiu, X.; Wang, C.; Yin, S.; Zeng, Q.; Xu, B.; Bai, C. *J. Phys. Chem. B* **2000,** *104*, 3570. (b) Qiu, X.; Wang, C.; Zeng, Q.; Xu, B.; Yin, S.; Wang, H.; Xu, S.; Bai, C. *J. Am. Chem. Soc.* **2000**, *122*, 5550.

(14) Lei, S.; Wang, C.; Wan, L.; Bai, C. *J. Phys. Chem. B* **2004**, *108*, 1173.

(15) Yokoyama, T.; Yokoyama, S.; Kamikado, T.; Mashiko, S. *J. Chem. Phys.* **2001**, *115*, 3814.

(16) Lackinger, M.; Hietschold, M. *Surf. Sci.* **2002**, *520*, L619.

(17) Strohmaier, R.; Ludwig, C.; Petersen, J.; Gompf, B.; Eisenmenger, W. *J. Vac. Sci. Technol., B* **1996**, *14* (2), 1079.

(18) Barlow, D. E.; Hipps, K. W. *J. Phys. Chem. B* **2000**, *104*, 5993.

(19) Lackinger, M.; Müller, T.; Gopakumar, T. G.; Müller, F.; Hietschold, M.; Flynn, G. W. *J. Phys. Chem. B* **2004**, *108*, 2279.

(20) Day, P. N.; Wang, Z.; Pachter, R. *J. Mol. Struct. (THEOCHEM)* **1998**, *455*, 33.

(21) Tada, H.; Morioka, T.; Koma, A. *J. Phys.: Condens. Matter* **1994**, *6*, 1881−1892.

(22) Yanagi, H.; Ashida, M.; Elbe, J.; Woehrle, D. *J. Phys. Chem.* **1990**, *94*, 7056−7061.

(23) Yanagi, H.; Kouzeki, T.; Ashida, M. *J. Appl. Phys.* **1993**, *73*, 3812−3819.

(24) Hoshino, A.; Isoda, S.; Kurata, H.; Kobayashi, T. *J. Appl. Phys.* **1994**, *76*, 4113−4120.

(25) Reiter, M. M.; Jamitzky, F.; Trixler, F.; Heckl, W. M. *Phys. Status Solidi A* **2001**, *187*, 171−176.

(26) Hooks, D. E.; Fritz, T.; Ward, M. D. *Adv. Mater.* **2001**, *13*, 227−241.

(27) Whitesides, G. M.; Mathias, J. P.; Seto, C. T. *Science* **1991**, *254*, 1312.

(28) Suto, K.; Yashimoto, S.; Itaya, K. *J. Am. Chem. Soc.* **2003**, *125*, 14976.

(29) Walzer, K.; Hietschold, M. *Surf. Sci.* **2001**, *471*, 1.

(30) Leznoff, C. C., Lever, A. B. P.; Eds. *Phthalocyanines: Properties and Applications*; VCH Publishers: New York, 1989.

(31) Lovinger, A. J.; Forrest, S. R.; Kaplan, M. L.; Schmidt, P. H.; Venkatesan, T. *J. Appl. Phys.* **1984**, *55*, 476.

(32) Güntherodt, H.-J., Wiesendanger, R., Eds. *Scanning Tunneling Microscopy I*, 2nd ed.; Springer-Verlag: Berlin, Germany, 1994.

(33) Hunter, C. A.; Sanders, J. K. M. *J. Am. Chem. Soc.* **1990**, *112*, 5525.

(34) Miao, Q.; Nguyen, T.-Q.; Someya, T.; Blanchet, G. B.; Nuckolls, C. *J. Am Chem. Soc.* **2003**, *125*, 10284.

(35) Lee, W. K.; Heiney, P. A.; McCauley, J. P., Jr.; Smith, A. B. *Mol. Cryst. Liq. Cryst.* **1991**, *198*, 273.

(36) Arikainen, E. O.; Boden, N.; Bushby, R. J.; Lozman, O. R.; Vinter, J. G.; Wood, A. *Angew. Chem., Int. Ed.* **2000**, *39*, 2333.

(37) Claessens, C. G.; Stoddart, J. F. *J. Phys. Org. Chem.* **1997**, *10*, 254.

(38) Yanagi, H.; Ikuta, K.; Mukai, H.; Shibutani, T. *Nano Lett.* **2002**, *2*, 951.